R Values in Low Energy e^+e^- Annihilation

Zhengguo Zhao
Institute of High Energy Physics
Chinese Academy of Sciences
Beijing 100039, P.R. of China

1 Introduction

According to the quark-parton model, the production of hadrons via e^+e^- collisions is described by the annihilation of e^+e^- pairs into a virtual γ or Z^0 boson. In the lowest order, one defines the ratio of the rate of hadron production to that for muon pairs as

$$R \equiv \frac{\sigma(e^+e^- \to \text{hadrons})}{\sigma(e^+e^- \to \mu^+\mu^-)} = 3\sum_f Q_f^2, \tag{1}$$

where Q_f is the fractional charge of the quark, and the factor of 3 in front counts the three colors for each flavor. The cross section of the pure QED process is $\sigma(e^+e^- \to \mu^+\mu^-) = 4\pi\alpha^2/3s$. The value of R, which counts directly the number of quarks, both flavor and colors, is expected to be constant so long as the center-of-mass (cm) energy of the annihilated e^+e^- does not overlap with resonances or thresholds for the production of new quark flavors. One has

$$\begin{aligned} R &= 3[(2/3)^2 + (1/3)^2 + (2/3)^2] = 2 \quad \text{for} \quad u, d, s \\ &= 2 + 3(2/3)^2 = 10/3 \quad \text{for} \quad u, d, s, c, \\ &= 10/3 + 3(1/3)^2 = 11/3 \quad \text{for} \quad u, d, s, c, b. \end{aligned}$$

These values of R are only based on the leading order process $e^+e^- \to q\overline{q}$. However, one should also include the contributions from diagrams where the quark and anti-quark radiate gluons. The higher order QCD corrections to R have been calculated in complete third order perturbation theory [1], and the results can be expressed as

$$R = 3\sum_f Q_f^2 \left[1 + (\frac{\alpha_s(s)}{\pi}) + 1.411(\frac{\alpha_s(s)}{\pi})^2 - 12.8(\frac{\alpha_s(s)}{\pi})^3 + \ldots\right], \tag{2}$$

where $\alpha_s(s)$ is the strong coupling constant. Precise measurement of R at higher energy can be employed to determine $\alpha_s(s)$ according to Eq. (2), which exhibits a QCD correction known to $O(\alpha_s^3)$. In addition, non-perturbative corrections could be important at low cm energy, particularly in the resonance region.

R has been measured by many laboratories in the energy region from hadron production threshold to the Z^0 pole, and recently to the energy of W pair production [2]. The experimental R values are in general consistent with theoretical predictions, which is an impressive confirmation of the hypothesis of the three color degrees of freedom for quarks. The measurements of R in the low energy region were performed 15 to 20 years ago in Novosibirsk, Orsay, Frascati, SLAC, and Hamburg [3, 4, 5, 6, 7, 8, 9]. Figure 1 [10] shows the R values for cm energies up to 10 GeV, including resonances. For cm energies below 5 GeV, the uncertainties in R values are about 15% on average; and the structure in the charm threshold region is not well determined. The DASP group [11] inferred the existence of narrow resonances at 4.04 GeV and 4.16 GeV. In addition to the resonance at 3.77 GeV, Mark I data [12] shows broad enhancements at 4.04, 4.2, and 4.4 GeV. The resonance at 4.4 GeV was also observed by PLUTO [13], but the height and width of the resonance were reported differently. A new cross section measurement in the charm threshold region is needed to clarify the structure, which is important not only for the precision determination of $\alpha(M_Z^2)$ and the interpretation of the $(g-2)_\mu$ measurement of E821 at BNL, but also for the understanding of charmonium itself.
Between the charm and bottom thresholds, in the region 5–10.4 GeV, R was measured by Mark I, DASP, PLUTO, Crystal Ball, LENA, CLEO, CUSB, and DESY-Heidelberg collaborations. Their systematic normalization uncertainties were about 5-10%. Above bottom threshold, the measurements were made at PEP, PETRA, and LEP with uncertainties of 2-7%.

Place	Ring	Detector	E_{cm} (GeV)	Points	Year
Beijing	BEPC	BES II	2.0–5.0	85	1998–1999
Novosibirsk	VEPP-2M	CMD-2	0.6–1.4	128	1997–1999
		SND			
	VEPP-2	Olya,ND CMD	0.3–1.4		
SLAC	Spear	MarkI	2.8–7.8	78	1982
Frascati	Adone	$\gamma\gamma$2,MEA	1.42–3.09	31	1978
		Boson,BCF			
Orsay	DCI	M3N,DM1,DM2	1.35–2.13	33	1978
Hamburg	Doris	DASP	3.1–5.2	64	1979
		PLUTO	3.6–4.8	27	1977

Table 1: Measurements of R at low energy by different laboratories.

Remarkable progress has been made in the precision tests of the Standard Model (SM) during the last decade. The electroweak data from LEP is so copious and

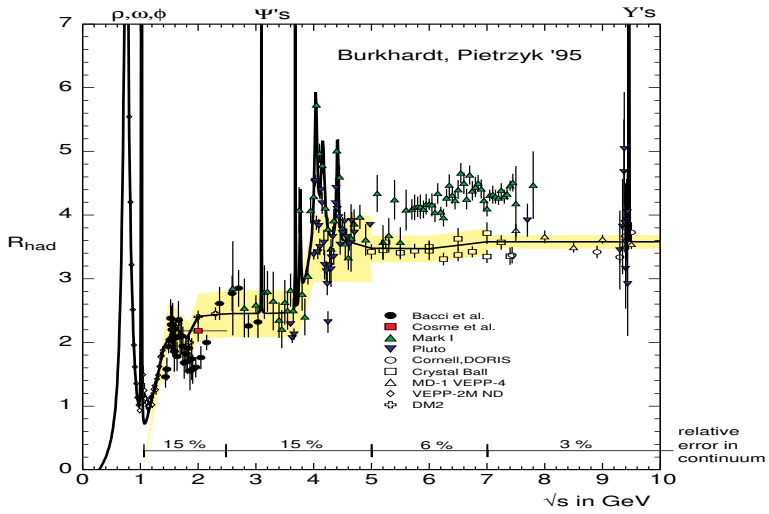

Figure 1: Experimental R values in the energy region below 10 GeV, from [10]. The relative errors on R in the continuum is given in numbers at the bottom of the figure.

precise that one can make use of the radiative correction effects to test the SM. In particular, the indirect determination of m_H depends critically on the precision of $\alpha(M_Z^2)$. Recently, for example, there has been an increasing interest from electroweak phenomenology to reduce the uncertainty in $\alpha(M_Z^2)$, which seriously limits further progress in the determination of the Higgs mass from radiative corrections to the SM [10, 14, 15, 16, 17, 18]. The uncertainty in $\alpha(M_Z^2)$ arises from the contribution of light quarks to the photon vacuum polarization $\Delta\alpha(s) = -\Pi'_\gamma(s)$ at the Z mass scale. This contribution is independent of any particular initial or final state and can be absorbed in $\alpha(s) \equiv \alpha/[1 - \Delta\alpha(s)]$, where α is the fine structure constant, $\alpha = 1/137.035\ 989\ 5(61)$. The correction $\Delta\alpha = \Delta\alpha_{\rm lepton} + \Delta\alpha_{\rm had}$. Of these, the leptonic part is precisely calculated analytically according to perturbation theory, because free lepton loops are affected only by small electromagnetic corrections [19]. However, the hadronic part $\Delta\alpha_{\rm had}$ cannot be entirely calculated from QCD because of ambiguities in defining the light quark masses m_u and m_d as well as the inherent non-perturbative nature of the problem at small energy scales, where the free quark loops are strongly modified by strong interactions at low energy. An ingenious way to handle this [19] is to relate $\Delta\alpha_{\rm had}$ from the quark loop diagram to R, making use of unitarity and analyticity,

$$\Delta\alpha^{(5)}_{\rm had}(s) = -\frac{s}{4\pi^2\alpha}P\left(\int_{4m_\pi^2}^{E^2_{\rm cm}} ds' \frac{R^{\rm data}(s')}{s'(s'-s)} + \int_{E^2_{\rm cm}}^{\infty} ds' \frac{R^{PQCD}(s')}{s'(s'-s)}\right), \qquad (3)$$

where $R(s) = \sigma(e^+e^- \to \text{hadrons})/\sigma(e^+e^- \to \mu^+\mu^-)$ and P is the principal value of the integral.

Much independent work has recently been done to evaluate $\alpha(s)$ at the energy of

the Z pole. So far, the uncertainty of $\Delta\alpha(s)$ is dominanted by the R values at low energy ($E_{\rm cm} < 5\ GeV$). These are measured with an average uncertainty of ~15%, as indicated in Fig. 1.

The anomalous magnetic moment of the muon $a_\mu \equiv (g-2)/2$ receives radiative contributions that can in principle be sensitive to new degrees of freedom and interactions. Theoretically, a_μ is sensitive to large energy scales and very high order radiative corrections. It therefore provides an extremely clean test of electroweak theory and may give us hints on possible deviations from the SM. The experimental and the theoretical predictions on a_μ are well reviewed by Roberts in his talk given at LP99 [20].

One can decompose a_μ as

$$a_\mu^{SM} = a_\mu^{QED} + a_\mu^{\rm had} + a_\mu^{\rm weak} \ . \tag{4}$$

The largest term, the QED contribution $a_\mu^{\rm QED}$, has been calculated to $O(\alpha^5)$, including the contribution from τ vacuum polarization. $a_\mu^{\rm weak}$ includes the SM effects due to virtual W, Z, and Higgs particle exchanges. $a_\mu^{\rm had}$ denotes the virtual hadronic (quark) contribution determined by QCD, part of which corresponds to the effects representing the contribution of the running of $\alpha(s)$ from low energy to a high energy scale. This term cannot be calculated from first principles but can be related to the experimentally determined $R(s)$ through the expression

$$a_\mu^{\rm had} = (\frac{\alpha m_\mu}{3\pi})^2 \int_{4m_\pi^2}^{\infty} ds \frac{R(s)K(s)}{s^2} \ , \tag{5}$$

where $K(s)$ is a kernel varying from 0.63 at $s = 4m_\pi^2$ to 1.0 at $s = \infty$.

The hadronic vacuum polarization is the most uncertain of all the SM contributions to a_μ. The uncertainty is presently 156×10^{-11}. For several scenarios, it has been claimed that "the physics achievement of the effort to measure the cross section of $e^+e^- \to$ hadrons that brings down the uncertainty of a_μ to 60×10^{-11} is equivalent to that of LEP2 or even the LHC" [21].

From Eqs. (3) and (5) one finds that $a_\mu^{\rm had}$ is more sensitive to lower energies than higher ones. Further measurements in the energy region of 0.5–1.5 GeV from VEPP-2M in Novosibirsk and DAΦNE in Frascati will contribute to the interpretation of the a_μ measurement at Brookhaven [22] and the luminosity measurement at CERN [14]. However, their contribution to the precision determination of $\alpha(M_Z^2)$ is limited. The improved R value from BES II at BEPC in the energy region of 2–5 GeV will make the major contribution to evaluate $\alpha(M_Z^2)$, and also partly contribute to the interpretation of a_μ.

2 Recent measurements of R in low energy e^+e^-

There are two different approaches to the measurement of R. One is to study the exclusive hadronic final states, *i.e.*, to measure the production cross section of each individual channel contributing to $\sigma(e^+e^- \to \text{hadrons})$. The value of R can then be obtained by summing over the measured hadron production cross sections of all individual channels. This method demands that the detector has good particle identification and requires the understanding of each channel. It is usually used for cm energies below 2 GeV.

Another method treats the hadronic final states inclusively. It measures R by dealing with all the hadronic events simultaneously and is suitable in an energy region where a reliable event generator for hadron production is available. With an improved Lund Model [23], we may be able to extend this region down to 2 GeV.

The typical features of hadron production below 5 GeV are:

• the presence of many resonances, such as, ρ, ω, φ, ρ', ω', φ', J/ψ, $\psi(2S)$, and resonances of D^+D^-, $D_s^+D_s^-$, and baryon-antibaryon

• a small number of final states and low charged multiplicity, usually $N_{\rm ch} \leq 6$.

The experimental challenge here is how to subtract the beam-associated background and select $N_{\rm had}$.

In the following section, I will first discuss some new measurements done by CMD-2 and SND at VEPP-2M in Novosibirsk, which are based on an exclusive analysis of the hadron production in the energy region around 0.4–1.4 GeV. Then, I will concentrate on discussing the R scan done by BES II at BEPC in Beijing in the energy region from 2–5 GeV, which measures R values by dealing with hadronic final states inclusively.

2.1 Recent results from VEPP-2M

VEPP-2M, an e^+e^- collider with maximum luminosity of $\sim 5 \times 10^{30}$ cm^{-2}s^{-1} at $E_{\rm beam}$=510 MeV, has been operating since 1974 in the energy region $E_{\rm cm}$ =0.4–1.4 GeV (ρ, ω, ϕ-meson region). SND [24] and CMD-2 [25] are the two detectors carrying out experiments at VEPP-2M. Since 1994, VEPP-2M has performed a series of scans from 0.38 GeV to 1.38 GeV [26]. With this data, both SND and CMD-2 have measured the cross sections for the channels $\pi^+\pi^-$, $\pi^+\pi^-\pi^0$, $\pi^+\pi^-\pi^+\pi^-$, $\pi^+\pi^-\pi^0\pi^0$, and $\pi^+\pi^-\pi^+\pi^-\pi^0$, as well as K_LK_S and K^+K^-.

Study of $e^+e^- \to \pi^+\pi^-\pi^+\pi^-, \pi^+\pi^-\pi^0\pi^0$

The four pion final states produced via e^+e^- annihilation in the $E_{\rm cm} = 1 \sim 2$ GeV energy region dominate and determine the main part of the hadronic contribution to a_μ and the QCD sum rules. These processes are also important sources of information for the understanding of hadron spectroscopy, in particular for the study of the

ρ-meson radial excitation [27]. These processes were studied at the VEPP-2M, DCI and ADONE colliders [28, 29, 30, 31, 32]. The statistical errors of these measurements were $\sim 5\%$, and the systematic errors were $\sim 15\%$. There was about a 20% discrepancy among the different experiments.

For the process of $e^+e^- \to \pi^+\pi^-\pi^+\pi^-$, the systematic error from the recent SND results is $\sim 7\%$, mainly coming from the event selection and the luminosity determination. The measured total cross sections from CMD-2 for $e^+e^- \to 2\pi^+2\pi^-$ are also illustrated in Fig. 2. Only the statistical errors are shown. The systematic uncertainties are $\sim 7\%$, attributed to the luminosity measurement, the event reconstruction and selection and also the radiative correction.

For SND, the backgrounds to the $e^+e^- \to \pi^+\pi^-\pi^0\pi^0$ channel are mainly from $e^+e^- \to K^+K^-$, QED processes $e^+e^- \to e^+e^-e^+e^-$, $e^+e^-\gamma\gamma$, and cosmic rays and beam associated background. The systematic error is $\sim 7\%$, of which $\sim 5\%$ arise from the variations of the detection efficiency. This is shown from the simulation of the intermediate states such as $\omega\pi^0$, $\rho^0\pi^0\pi^0$ and of hadron production with Lorentz-invariant phase space (LIPS).

The total cross section for $e^+e^- \to \pi^+\pi^-2\pi^0$ process measured by CMD-2 also is plotted in Fig. 3. The error bars indicate only the statistical error. The systematic uncertainties mainly come from event reconstruction, radiative corrections, and the luminosity determination. The overall systematic uncertainty is estimated to be 7%. The cross section measured by this experiment is consistent with what was measured by OLYA [33] and a recent result from SND [34]. However, the cross section from all three measurements is apparently lower than that given by ND [35, 36]. For comparison, the results from Orsay and Frascati above 1.4 GeV are also shown in the figure.

CMD-2 finds that the dominant contribution to the cross section of the process $e^+e^- \to \pi^+\pi^-2\pi^0$ comes from $\omega\pi^0$ and $\rho^\pm\pi^\mp\pi^0$ intermediate states, whereas the $\rho^0\pi^0\pi^0$ state is not observed. The $\rho^\pm\pi^\mp\pi^0$ states are saturated completely by the $a_1(1260)\pi$ intermediate state. This is also the dominant contribution to the cross section for the process $e^+e^- \to 2\pi^+2\pi^-$. The theoretical predictions for the differential distributions and the total cross sections can be dramatically changed if one takes into account the interference of different amplitudes with various intermediate states, but identical final states.

The cross section for $e^+e^- \to 4\pi$ can be related to the four π decays of the τ-lepton through the hypothesis of CVC [16]. This has been experimentally tested to be valid within an accuracy of 3–5% [37]. The observed $a_1(1260)\pi$ dominance, if it is true, should be taken into account in τ decays.

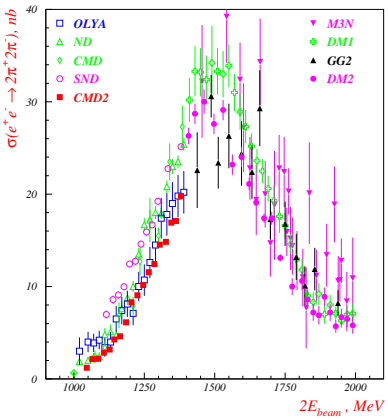

Figure 2: Energy dependence of the cross section of $e^+e^- \to 2\pi^+2\pi^-$.

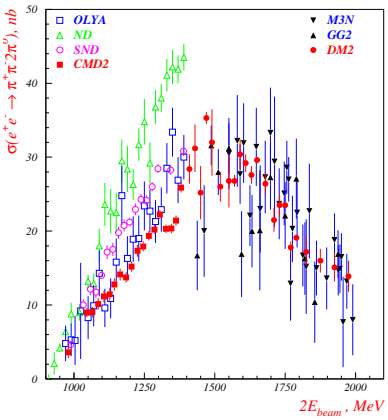

Figure 3: Energy dependence of the cross section of $e^+e^- \to \pi^+\pi^-2\pi^0$.

The investigation of $e^+e^- \to \pi^+\pi^-\pi^0$

This process was measured by ND at VEPP-2M in the energy region up to 1.1 GeV [38]. The measured cross section is significantly higher than that predicted by the Vector Dominance Model (VDM). However, it is well known that the VDM is able to well describe the cross section near the ω and ϕ resonances for the processes $e^+e^- \to \omega,\ \phi \to \rho\pi \to \pi^+\pi^-\pi^0$. It is therefore necessary to perform new precise measurements in the non-resonant region to investigate the limitations of the VDM and determine possible contributions from heavier intermediate states like $\omega(1120)$ or $\omega(1600)$.

SND also measured this channel. The systematic errors from the detection efficiency, luminosity measurement, and the background subtraction were 10%, 5% and 5%, respectively, giving a total systematic error of $\sim$ 12%. The results from the new measurement agree with the old ND data.

Invariant masses of π-meson pairs in the final 3π state were measured to investigate the intermediate state in the $e^+e^- \to \pi^+\pi^-\pi^0$ process. The possible intermediate states are $\rho\pi$ and, much less probably, $\omega\pi$ with decay $\omega \to 2\pi$. Comparing the mass spectrum of $\pi^+\pi^-$ with that of $\pi^0\pi^\pm$, one can observe the interference between the two intermediate states. The clear peak shown in $\pi^+\pi^-$ mass spectrum of the experimental data proves the $\rho - \omega$ interference in 3π final state, and the phase is measured to be zero in agreement with the VDM prediction. Figure 4 plots the cross section for the production of $\pi^+\pi^-\pi^0$.

Cross section measurement for $e^+e^- \to K_SK_L$

The cross section of $e^+e^- \to K_SK_L$ reaction was measured in 1982 by OLYA in Novosibirsk [39] and DM1 in Orsay [40], in the energy regions $E_{\rm cm}$ = 1.06–1.40 GeV

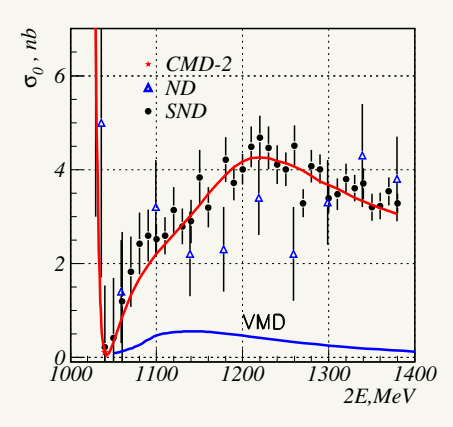

Figure 4: Energy dependence of the cross section of $e^+e^- \to \pi^+\pi^-\pi^0$. The solid line shows the VDM prediction.

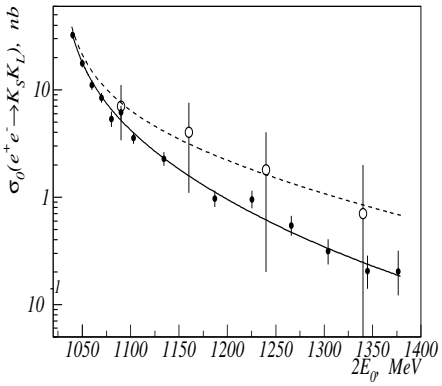

Figure 5: Energy dependence of the cross section of $e^+e^- \to K_SK_L$. The solid dots are from SND.

and $E_{\rm cm}$ = 1.40–2.20 GeV respectively. It is desirable to re-measure this channel, because the accuracy reached by both experiments is poor. So far, 1.8 pb^{-1} data has been analyzed by SND, utilizing $K_S \to \pi^0\pi^0$ from $e^+e^- \to K_SK_L$. The reaction $e^+e^- \to \omega\pi^0 \to \pi^0\pi^0\gamma$ is the main background source. In addition, cosmic rays and beam associated background also contribute. The cross section measured by SND is shown as the solid dots in Fig. 5.

$\boldsymbol{e^+e^- \to \omega\pi^+\pi^-}$ ($\boldsymbol{\omega \to \pi^+\pi^-\pi^0}$), $\boldsymbol{\eta\pi^+\pi^-}$ ($\boldsymbol{\eta \to \pi^+\pi^-\pi^0}$, or $\boldsymbol{\gamma\gamma}$)

Figures 6 and 7 plot the cross section measured by CMD-2 for $\omega\pi^+\pi^-$ and $\eta\pi^+\pi^-$, together with the measurement by DM2. The new measurement significantly reduced the uncertainties, though the systematic errors are still as high as 15%.

$\boldsymbol{e^+e^- \to \pi^+\pi^-}$

The cross section for the process $e^+e^- \to \pi^+\pi^-$ is given by

$$\sigma = \frac{\pi\alpha^2}{3s}\beta_\pi^3|F_\pi(s)|^2, \tag{6}$$

where $F_\pi(s)$ and β_π are, respectively, the pion form factor at the cm energy $\sqrt{s}$ and the velocity of the pion. A precision measurement of the pion form factor is necessary to determine the R values via an exclusive method. The uncertainty in the hadronic contribution to a_μ is dominated by the $e^+e^- \to \pi^+\pi^-$ channel with $\sqrt{s} < 2$ GeV [16, 37]. The experiment E821 at BNL [20] has measured a_μ to a precision of ~ 5 ppm and will further improve the accuracy to about 1 ppm. In order to compare

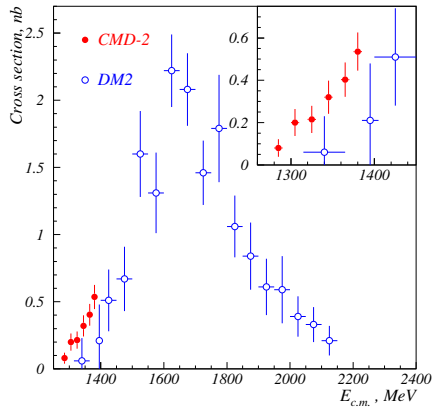

Figure 6: Cross sections for the reaction $e^+e^- \to \omega\pi^+\pi^-$ (with $\omega \to \pi^+\pi^-\pi^0$).

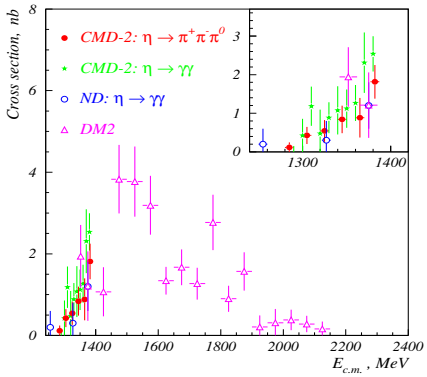

Figure 7: Cross section for $e^+e^- \to \eta\pi^+\pi^-$ (with $\eta \to \pi^+\pi^-\pi^0$ or $\gamma\gamma$).

a measurement with such a high accuracy with theory, the uncertainty in R should be below 0.5% in this energy region. A new measurement of the pion form factor with smaller uncertainty is important for the interpretation of this measurement.

The pion form factor was measured by the OLYA and CMD groups at VEPP-2M about twenty years ago [41]. Twenty-four points from 360 to 820 MeV were studied by CMD with a systematic uncertainty of about 2%. The OLYA measurement scanned from 640 to 1400 MeV with small steps, giving a systematic uncertainty from 4% at the ρ-meson peak to 15% at 1400 MeV.

The pion form factor is one of the major experiments planned at CMD-2. A total of 128 energy points were scanned in the whole VEPP-2M energy region (0.36–1.38 GeV) in six runs performed from 1994 to 1998 [26]. The discussion here is based on data taken from the first 3 runs with 43 energy points ranging from 0.61–0.96 GeV. The small energy scan step, 0.01 GeV, in this energy region allows the calculation of the hadronic contribution in a model-independent way. In order to investigate the ω-meson parameters and the $\rho - \omega$ interference, the energy steps were 2–6 MeV in the energy region near the ω-meson. The beam energy was measured with the resonance depolarization technique for almost all of the energy points, which significantly reduced the systematic error arising from the energy uncertainty. The charged trigger made use of the information from the drift chamber and the Z-chamber and required at least one track. There was an additional trigger criteria for the energy points between 0.81 and 0.96 GeV, which asked for the total energy deposited in the calorimeter to be greater than 20–30 MeV. The neutral trigger, reserved for monitoring the trigger efficiency, is based on the information only from the calorimeter.

The background is mainly from cosmic muons. Bhabha and dimuon production are also background sources. The shape of the energy deposition was carefully studied for

the event separation and selection. An event vertex cut was applied to reject cosmic muons effectively.

To account for the fact that the radiative correction to $e^+e^- \to \pi^+\pi^-$ depends on the energy behavior of the cross section of $e^+e^- \to \pi^+\pi^-$ itself, the radiative correction factor was calculated iteratively. The existing $|F_\pi(s)|^2$ data were used as the first iteration for the calculation. The values of $|F_\pi(s)|^2$ were found to be stable after three iterations.

The corrections for the pion losses due to decays in flight and nuclear interaction, as well as the background from $\omega \to 3\pi$ were done using Monte Carlo simulations.

The total systematic uncertainty was estimated to be currently 1.5% and 1.7% for the energy region 0.78–0.784 GeV and 0.782–0.94 GeV, respectively, and 1.4% for all the other points.

Beyond the leading contributions from $\rho(770)$ and $\omega(782)$, the resonances $\rho(1450)$ and $\rho(1700)$ should be taken into account to describe the data for the determination of the pion form factor. In addition, the model based on the Hidden Local Symmetry (HLS), which predicts a point-like coupling $\gamma\pi^+\pi^-$, can describe the experimental data well in the region below 1 GeV. Both the Gounaris-Sakurai (GS) parameterization and the HLS parameterization approaches [41, 42] were used to fit the form factor. Of the higher resonances, only $\rho(1450)$ was taken into account in fitting the pion form factor in the relatively narrow energy region 0.61–0.96 GeV. Figure 8 shows the fit of the pion form factor with CMD-2 94, 95 data according to GS and HLS models. The two theoretical curves are indistinguishable.

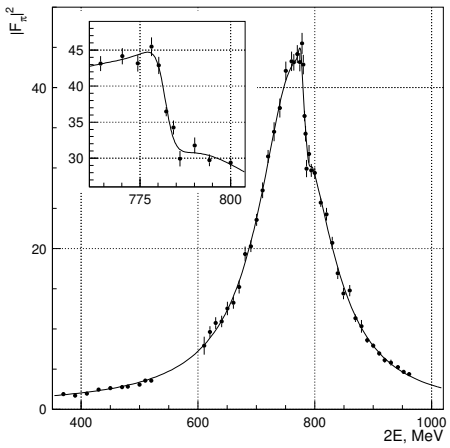

Figure 8: Pion form factor measured by CMD-2.

The pion form factor fit of the CMD-2 94, 95 data is summarized in Table 2. With the remaining data collected, CMD-2 hopes to reduce the systematic error presented here by a factor of two. To achieve this goal, a new approach for the calculation of the radiative correction must be developed.

	GS model	HLS model
M_ρ (MeV)	775.28±0.61±0.20	774.57±0.60±0.20
Γ_ρ (MeV)	147.70±1.29±0.40	147.65±1.38±0.20
$Br(\omega \to \pi^+\pi^-)$,%	1.31±0.23±0.02	1.32±0.23±0.02
β(GS)	-0.0849 ± 0.0053 ±0.0050	–
α(HLS)	–	2.381±0.016±0.016
χ^2/n	0.77	0.78

Table 2: The results of fit of the CMD-2 94, 95 pion form factor data by the GS and HLS models.

2.2 R scan with BES II at BEPC in Beijing

With an upgraded machine and detector [43, 44, 45], the BES collaboration performed two scans to measure R in the energy region of 2–5 GeV in 1998 and 1999. The first run scanned 6 energy points covering the energy from 2.6 to 5 GeV in the continuum. Separated beam running at each energy point was carried out in order to subtract the beam associated background from the data [45].
The second run scanned about 85 energy points in the energy region of 2–4.8 GeV [46]. To subtract beam associated background, separated beam running was done at 26 energy points and single beam running for both e^- and e^+ was done at 7 energy points distributed over the whole scanned energy region. Special runs were taken at the J/ψ to determine the trigger efficiency. The J/ψ and $\psi(2S)$ resonances were scanned at the beginning and at the end of the R scan for energy calibration.
The R values are measured from the BES II scan data by observing the final hadronic events inclusively. That is, the value of R is determined from the number of observed hadronic events ($N_{\rm had}^{\rm obs}$) by the relation

$$R = \frac{N_{\rm had}^{obs} - N_{\rm bg} - \sum_l N_{ll} - N_{\gamma\gamma}}{\sigma_{\mu\mu}^0 \cdot L \cdot \epsilon_{\rm had} \cdot \epsilon_{\rm trg} \cdot (1+\delta)}, \tag{7}$$

where $N_{\rm bg}$ is the number of beam associated background events; $\sum_l N_{ll}$, $(l = e, \mu, \tau)$ and $N_{\gamma\gamma}$ are the numbers of misidentified events from one-photon lepton pair and two-photon processes, L is the integrated luminosity, δ is the radiative correction, $\epsilon_{\rm had}$ is the detection efficiency for hadronic events, and $\epsilon_{\rm trg}$ represents the trigger efficiency. The trigger efficiencies are measured by comparing the responses to different trigger requirements in special runs taken at the J/ψ resonance. From the trigger measurements, the efficiencies for Bhabha, dimuon, and hadronic events are determined to be 99.96%, 99.33%, and 99.76%, respectively. As a cross check, the trigger information from the 2.6 and 3.55 GeV data samples is used to provide an independent measurement of the trigger efficiencies. This measurement is consistent with the efficiencies

determined from the J/ψ data. The errors in the trigger efficiencies for Bhabha and hadronic events are less than 0.5%.

The task of the hadronic event selection is to identify one photon multi-hadron production from all possible contamination mechanisms. The event selection makes full use of all the information from each sub-detector of BES II, namely, the vertex position, the measured charged-particle momentum, the energy loss due to ionization, the related time of flight, the associated pulse height and pulse shape of the electromagnetic calorimeter, and the hits in the μ counter.

The backgrounds involved in the measurement are mainly from cosmic rays, lepton pair production (e^+e^-, e^+e^-, $\mu^+\mu^-$, $\tau^+\tau^-$), two-photon processes, and beam associated processes. The cosmic rays and part of the lepton pair production events are directly removed by the event selection. The remaining background from lepton pair production and two-photon processes is then subtracted out statistically according to a Monte Carlo simulation.

The beam associated background sources are complicated. They may mainly come from beam-gas and beam-wall interaction, synchrotron radiation, and lost beam particles. The salient features of the beam associated background are that their tracks are very much along the beam pipe direction, the energy deposited in BSC is small, and most of the tracks are protons.

Separated-beam runs were performed for the subtraction of beam associated background. Most of the beam associated background events are rejected by vertex and energy cuts. Applying the same hadronic events selection criteria to the separated-beam data, one can obtain the number of separated-beam events $N_{\rm sep}$ surviving these criteria. The number of beam associated events $N_{\rm bg}$ in the corresponding hadronic event sample is given by $N_{\rm bg} = f \cdot N_{\rm sep}$, where f is the ratio of the product of the pressure at the collision region times the integrated beam currents for colliding beam runs and that for the separated beam runs. To subtract beam associated background in this way, the variation of the pressure in the collision region and the beam current must be recorded for both colliding and separated-beam runs at each energy to be measured.

JETSET 7.4 is used as the hadronic event generator to determine the detection efficiency for hadronic events. Parameters in the generator are tuned using a 4×10^4 hadronic event sample collected near 3.55 GeV for the tau mass measurement done by the BES collaboration [47]. The parameters of the generator are adjusted to reproduce distributions of kinematic variables such as multiplicity, sphericity, and transverse momentum.

The parameters have also been obtained using the 2.6 GeV data ($\approx 5 \times 10^3$ events). The difference between the two parameter sets and between the data and the Monte Carlo data based on these parameter sets is used to determine a systematic error of 1.9–3.2% in the hadronic efficiency.

The Monte Carlo simulation package JETSET was not designed to fully describe few

body states produced by e^+e^- annihilation in the few GeV energy region, though the event shapes are consistent with that from the Monte Carlo simulation with parameters tuned at 3.5 GeV. A great effort has been made by the Lund group and the BES collaboration to develop, directly for the Monte Carlo simulation, a formalism using the basic Lund Model area law which is expected to describe the data better [23].

Radiative corrections were determined using four different schemes [48, 49, 50, 51], which agreed with each other to within 1% below charm threshold. Above charm threshold, where resonances are important, the agreement is within 1–3%. The major uncertainties common to all models are due to errors in previously measured R values and in the choice of values for the resonance parameters. For the measurements reported here, we use the formalism of [50] and include the differences with the other schemes in the systematic error of 2.2–4.1%.

The R values obtained at the six energy points scanned in 1998 are shown in Table 3 and displayed graphically in Fig. 9 with solid dots. The largest systematic error is due to the hadronic event selection and is determined to be 3.8–6.0% by varying the selection criteria. The systematic errors on the measurements below 4.0 GeV are similar and are a measure of the amount of error common to all points. The BES collaboration has also performed the analysis including only events with greater than two charged tracks; although the statistics are smaller, the results obtained agree well with the results shown here.

$E_{\rm cm}$(GeV)	2.6	3.2	3.4	3.55	4.6	5.00
R	2.64	2.21	2.38	2.23	3.58	3.47
Stat. error	0.05	0.07	0.07	0.06	0.20	0.32
Sys. error	0.19	0.13	0.16	0.16	0.29	0.29

Table 3: R values measured with BES II from 1998 run.

The R values for $E_{\rm cm}$ below 4 GeV are in good agreement with results from $\gamma\gamma 2$ [7] and Pluto [9], but are below those from Mark I [8]. Above 4 GeV, our values are consistent with previous measurements.

Preliminary R values at 2.4, 2.5, 2.6, 2.7, 2.8, 2.9, 3.0, 4.6, and 4.8 GeV are plotted with solid squares in Fig. 10. The preliminary errors, which add the statistical and systematical errors in quadrature, are all conservatively assigned to be 10%. However, it is believed that these errors can be decreased to be comparable to the error bars of the solid dots, *i.e.* $\sim 7\%$ for the energy points below 3.6 GeV and $\sim 10\%$ for energies above 4.5 GeV. The first scan repeated the 3.4 GeV and the second scan repeated the 2.6 and 4.6 GeV data points measured in the first scan. In all cases, R values obtained are consistent with each other at the same energy.